Valence Bond Study of the SiH_3−F Bond

Harold Basch,* Joel L. Wolk, and Shmaryahu Hoz

Department of Chemistry, Bar Ilan University, Ramat Gan 52900, Israel

Received: November 6, 1996; In Final Form: March 26, 1997[⊗]

The binding energy curves of SiH_3−F have been investigated using *ab initio* valence bond self-consistent-field (VBSCF) methods. The atomic core electrons are treated both all-electron and by using an effective core potential (ECP) representation; for comparison and testing purposes. The VB wave function is expressed in terms of the covalent (SiH_3:F) and ionic ($SiH_3^+F^-$,$SiH_3^-F^+$) configurations, and the nonorthogonal orbitals are expanded in conventional atom-centered Gaussian basis sets. Several theory levels are applied, up to the use of different orbitals for different VB structures and allowing delocalization mixing among the passive SiH_3 and F fragment orbitals. Replacing the core electrons with an ECP is found to generally have a relatively small effect on the calculated ground state bond dissociation energy (BDE) curve, but a much larger effect on the individual covalent and ionic structure energy curves. Delocalization mixing is found to be important to achieving high accuracy for the equilibrium bond distance (R_e), BDE (D_e), and dipole moment of SiH_3F. The $SiH_3^+F^-$ ionic structure curve is found to lie below the covalent energy curve from at least R(C−F) = 1.3 Å out to ∼2.5 Å, but is stable relative to the dissociation asymptote by less than half of the ground state D_e. The magnitude of D_e in SiH_3−F is, therefore, determined by resonance coupling between the covalent and ionic structures (H_{12}), where the dominant VB structure at R_e is $SiH_3^+F^-$. The SiH_3:F covalent curve is found to be nearly as repulsive at its R_e value (1.59 Å) as previously found for CH_3:F at its R_e (1.38 Å). The proportionality constant K in the equation $H_{12} = KS_{12}[H_{11} + H_{22}]/2$, where H_{ij} and S_{ij} ($i, j = 1, 2$) are the Hamiltonian and overlap matrix elements, respectively, between the covalent and ionic configurations, has been evaluated using the results of these calculations. At the localized fragment theory level, K is found to be very close to 1 and remarkably constant over the range of R(Si−F) distances sampled here, independent of core representation and basis set.

1. Introduction

The proper description of bond dissociation energy curves is central to an accurate analysis of chemical reaction paths by theoretical methods. For the simple electron pair bond between radicals A• and B• the classical valence bond (VB) description, as elaborated for example by Pauling,[1] views this bond as being composed of a linear combination of perfectly covalent (A:B) and ionic (A^+B^-,A^-B^+) configurations. In this description all the electrons are localized on one of the two fragments A and B, with no electron delocalization between them. The nature of that bond is then discussed in terms of the relative weights or contributions of the covalent and ionic structures. This qualitative description can be refined and quantified using *ab initio* VB theories to produce accurate wave functions, energies and properties.[2−6] A significant advantage of the VB model for this type of bond is the correct homolytic dissociation of the bonding electron pair into radical fragments even at the simplest theoretical level. This capability is very important for treating chemical reaction paths.

Recent *ab initio* VB studies have focused on the simple MH_3−X (M = C,Si) and X−X molecules, where X is a substituent that is singly bonded to the methyl group.[7−11] The surprising result obtained is that for certain electron pair bonds, and even homopolar cases, the covalent configuration (MH_3:X and X:X) dissociation energy curves are found to be only mildly binding, or even repulsive, even when the overall bond dissociation energy (in MH_3−X, for example) is substantial. The tendency to weaker covalent component binding is found to correlate with the electronegativity of the binding atom in X; the higher the electronegativity, the smaller the covalent structure contribution. The more electronegative atoms also tend to have more nonbonding lone pairs of electrons. The small or nonexistent extent to which the covalent configuration contributes to the overall binding energy in these systems is unanticipated. The ground state electronic binding energy in these cases has been attributed to a strong resonance interaction between the ionic and covalent configurations, which converts a shallow or even repulsive lower energy covalent structure curve to a normal ground state Morse-type shape with a binding energy very close to the experimental value.[7,10] All these effects require further characterization and explanation.

An important aspect of the electron pair bond is its description as a function of row in the periodic table. It has been widely noted[1,11−13] that on going down the periodic table, for example from M = carbon to lead, the group 14 compounds MH_3−X can be divided into those whose bond dissociation energies (BDE) increase from M = carbon to silicon and those whose BDE decrease from M = carbon to silicon. These different trends also seem to correlate with the electronegativity of the bonding atom in X, where the more electronegative substituents (N, O, halogens) show increasing BDE from M = carbon to Si in MH_3−X. The origin of this dichotomy in BDE behavior needs to be elucidated.

In this regard, the simplest way to treat a valence isoelectronic series of compounds going down a column in the periodic table in *ab initio* electronic structure theory is to use effective core potentials to replace the chemically inert atomic core electrons. The effective potential method also allows the introduction of radial scaling relativistic effects on the valence electrons of the heavier atom, where they are most needed.[14−17] The use of effective core potentials (ECP) needs to be tested specially in *ab initio* VB theory because of the unique character of each of

[⊗] Abstract published in *Advance ACS Abstracts,* June 1, 1997.

S1089-5639(96)03715-2 CCC: $14.00

the contributing structures, which includes fully ionic configurations. This situation may be different from *ab initio* molecular orbital (MO) theory, where the electronic configurations are usually somewhere between purely covalent and fully ionic, in a mean field description.

We have therefore undertaken an *ab initio* VB electronic structure study of SiH_3F for the purposes of examining the SiH_3-F ground state energy dissociation curve, comparing properties with CH_3-F, and benchmark testing the ECP method within the VB framework. Particular interest is focused on the nature of the MH_3-F (M = C, Si) bond and its description both from the theoretical and experimental points of view.

2. Methods

All the nonorthogonal orbital VB calculations reported here were carried out using the TURTLE set of computer codes obtained from Dr. J. H. van Lenthe of Utrecht University and his collaborators[18]. The program carries out VB self-consistent-field (VBSCF) calculations on linear combinations of orbital configurations, where all possible spin-coupled determinental structures belonging to each VB configuration are generated. For the three configuration (SiH_3:F, $SiH_3^+F^-$, and $SiH_3^-F^+$) representation of the SiH_3-F bond there is only one VB structure for each configuration. The nonorthogonal VB orbitals are expanded in the usual atom-centered Gaussian basis sets. Both the VB structure and the orbital expansion coefficients are simultaneously VBSCF optimized. In order to carry out the ECP method calculations, stored atom potentials and the appropriate integral evaluation routines[14−17] were added to the TURTLE package.

The electronic ground state wave functions and energies for SiH_3-F were generated pointwise for the homolytic dissociation process from $R(Si-F) = 1.4$ Å to $R(Si-F) = 10$ Å, at internuclear distance (R) intervals of 0.1 Å out to 3.0 Å, and at larger intervals beyond that. The SiH_3 fragment geometry at each fixed R value was taken from the appropriate GVB[4] theory level optimization, distributing the SiH_3-F bond electron pair between two natural orbitals. Gaussian94[20] was used for the GVB calculations. This procedure was carried out separately for the all-electron (AE) core and ECP calculations. For benchmark and comparison purposes, a complete set of VBSCF bond dissociation energy curves was generated for each of three combinations of core representation and basis set: VBSCF-(ECP/ECP), VBSCF(ECP/AE), and VBSCF(AE/AE). In the first two sets the GVB(ECP/ECP) optimized geometries were used at each R value, and for the VBSCF(AE/AE) calculations the geometries were taken from the GVB(AE/AE) optimizations.

The ECP themselves and the valence electron basis sets for the Si and F atoms were taken from published tabulations.[16] The shared sp exponent ECP basis sets consist of four Gaussian primitives (4^{sp}) split 31 for fluorine and completely uncontracted for silicon. A single primitive sp set of diffuse Gaussians was added to F, taken from an even-tempered extension of the valence set. The actual exponent value is 0.0746. In addition, a single set of d-type polarization functions (five components) was added to the heavy atoms with exponents 0.4500 (Si) and 0.9000 (F). An unscaled triple-ζ contraction distribution (311) of the Huzinaga[21] 5^s basis set was taken for the hydrogen atom. For the AE basis set, Dunning's (6111/41) contraction[22] of Huzinaga's 9^s5^p atom optimized basis for the fluorine atom was augmented by a single primitive diffuse s and p set with Gaussian exponent values of 0.1093(s) and 0.0796(p). A set of single Gaussian d-type polarization functions (five components) was also added with exponent 0.9000. For the silicon atom the 6-311G(d) basis set of Pople *et al.*[23] as stored in Gaussian94[20] [$6^s5^p1^d$] was used. The same hydrogen atom basis set described above was also adopted for the AE/AE and ECP/AE calculations. Altogether, the ECP basis set consists of 47 basis functions and the AE set contains 54 functions.

At all the VB theory levels applied here the orbital electrons were divided into an active and a passive set. The passive electrons are in orbitals that are VBSCF variationally determined at each $R(SiH_3-F)$ distance and the GVB optimized geometry, with fixed double occupancy. The passive electrons are not correlated. The active set is correlated and consists only of the electron pair that forms the SiH_3-F bond. All the other electrons are in the passive category, and their exact number depends on the core representation: ECP or AE. The active pair of electrons is represented by the three VB configurations whose spatial forms are

$$[a(1)b(2) + b(1)a(2)] \tag{1a}$$

$$b'(1)b'(2) \tag{1b}$$

$$a'(1)a'(2) \tag{1c}$$

each multiplied by the usual spin-singlet function. Here, the orbitals a and a′ represent the bonding SiH_3 orbital, and b,b′ represent the bonding fluorine orbital. Equation 1a is the covalent (SiH_3:F) configuration, and (1b) and (1c) represent the ionic $SiH_3^+F^-$ and $SiH_3^-F^+$ configurations, respectively. Unlike the orbital split covalent configuration, the ionic configurations are always doubly occupied.[17]

The simplest VB model uses a common set of both passive and active VB orbitals for all three configurations. For the active set this means that a and a' are identical, and b and b′ are identical in eqs 1. The common orbital level is the classical VB method and can be denoted as SODS (same orbitals for different VB structures). All the passive and active VB orbitals are localized exclusively on either the SiH_3 or F fragments. The localization restriction is enforced by limiting the basis set space of each VB orbital to those basis functions belonging to the atom(s) only on one or the other of the fragments. all the VB orbitals are, thereby, necessarily nonorthogonal. Combining fragment localization with SODS gives the L-SODS model level. Altogether, 8 (ECP core) or 14 (AE core) VB orbitals are optimized at the SODS level.

The next level of treatment has been described by Verbeek, van Lenthe, Hiberty and co-workers.[3,11,24−26] Both the passive and active orbitals in the two ionic configurations, (1b) and (1c), are expected to be substantially different than in (1a). For example, the valence atomic orbitals in F^- and F^+ should be, respectfully, more and less diffuse than in the neutral fluorine atom. The differential relaxation effect for different charged species can be taken into account by allowing all the SiH_3 and F fragment orbitals to be different for each VB configuration. For the active orbitals in (1) this means that a′ is different from a and b′ is different from b, although the $\langle a|a'\rangle$ and $\langle b|b'\rangle$ overlaps can be very large. Independent energy optimization of a completely different set of fragment orbitals in the VBSCF for each configuration is a feature of the TURTLE programs package and fits naturally into the nonorthogonality of the VB orbitals. The different ionic structure ($SiH_3^+F^-$ and $SiH_3^-F^+$) orbitals have been called "breathing orbitals" and this level of theory termed BOVB.[3,11,24−26] Using such tailored orbitals for different VB structures (called TODS in ref 10 introduces dynamic correlation effects since it is equivalent to adding extravalent orbitals and excitations in a multiconfiguration expansion using orthogonal MOs.[3,27] The idea of optimizing different orbitals for each VB structure in a multielectron system was originally discussed by Goddard, *et al.*[28] and has been applied by others.[6,10,29,30] Within a purely localized fragment orbital basis this level is labeled L-BOVB.

TABLE 1: Calculated Equilibrium Si−F Bond Lengths (R_e), Dissociation Energies (D_e), Dipole Moments (μ) and VB Configuration Weights for the Three-Configuration VBSCF Calculations

	ground state				$SiH_3^+F^-$		
theory level[a]	R_e (Å)	D_e (kcal/mol)	μ[b] (D)	weight[c] SiH_3F	weight	R_e (Å)	D_e[g] (kcal/mol)
L-SODS(AE/AE)	1.667	108.2	2.062	0.4162	0.5988	1.667	31.5
D-SODS(AE/AE)	1.612	120.7	1.612	0.4159	0.6004	1.609	44.1
GVB	1.612	123.6	1.648				
L-BOVB(AE/AE)	1.662	129.2	1.930	0.4519	0.5832	1.749	42.9
D-BOVB(AE/AE)	1.609	143.0	1.437	0.4167	0.6221	1.686	57.0
L-SODS(ECP/AE)	1.670	107.5	2.049	0.4065	0.5994	1.761	22.1
D-SODS(ECP/AE)	1.615	120.3	1.610	0.4243	0.5823	1.742	27.7
L-BOVB(ECP/AE)	1.665	128.3	1.935	0.4399	0.5947	1.800	34.0
D-BOVB(ECP/AE)	1.610	141.6	1.477	0.4221	0.6138	1.745	46.8
L-SODS(ECP/ECP)	1.666	107.0	2.004	0.4410	0.5610	1.845	11.4
D-SODS(ECP/ECP)	1.612	119.9	1.596	0.4430	0.5600	1.792	18.8
GVB	1.607	122.8	1.596				
L-BOVB(ECP/ECP)	1.664	125.9	1.916	0.4761	0.5576	1.915	27.9
D-BOVB(ECP/ECP)	1.608	142.0	1.460	0.4481	0.6016	1.885	32.1
experimental	1.593[d]	155.9[e]	1.298[f]				

[a] See text for definitions. [b] Evaluated at the GVB energy minimum. [c] See eq 2. Weights don't add up to 1.0 because $SiH_3^-F^+$ is not listed and its weight has a small negative value in some cases. [d] From ref 32. [e] D_o from ref 33. [f] From ref 34. [g] Relative to ground state asymptotes.

An improved description of the VB wave function can be obtained by allowing interfragment delocalization mixing between the passive electrons only[3,10,11,24] at both the SODS (D-SODS) and BOVB (D-BOVB) levels. With such delocalization mixing, all the passive electrons are expanded in the combined SiH_3 + F basis sets in all the configurations irrespective of orbital symmetry, while the active electron pair orbitals are still fragment localized. Passive orbital delocalization is a stabilizing interaction, and, among other effects, in SiH_3−F it effectively introduces a degree of charge transfer (CT) from the fluorine lone pair electrons into the Si−H orbital space. This CT is already present in the $SiH_3^-F^+$ configuration, but interfragment passive electron delocalization increases the number of variational parameters at the basis function mixing level and introduces new CT effects.[3,10]

Relative to the simplest model level L-SODS, using tailored orbitals for different VB structures (L-BOVB) is variationally more effective than passive orbital delocalization (D-SODS). If D-SODS is taken one step further and the active orbitals are also allowed complete basis set mixing, then the three-configuration representation in eq 1 collapses to the one covalent structure GVB method, which includes only nondynamical correlation of the active electron pair.[4] Thus, based on the variational energies, the order of increasing accuracy is expected to be L-SODS < D-SODS < GVB < L-BOVB < D-BOVB. In the BOVB level calculations carried out here with the AE core, the fluorine 1s and silicon 1s to 2p core orbitals were optimized as a common set for all three VB configurations. Therefore, altogether 28 VB orbitals are variationally optimized at each R(Si−F) distance geometry. At the BOVB level with the CEP core representation the fluorine 1s and silicon 1s to 2p electrons are not treated explicitly and only 22 VB orbitals are optimized.

Due to the nonorthogonality of the VB orbitals, the weights of each VB structure (W_i, $i = 1-3$) are calculated from the structure expansion coefficients (C_i) from the formula[31]

$$W_i = C_i \sum_{j=1}^{3} S_{ij} C_j \qquad (2)$$

where S_{ij} is the overlap between VB structures. This relationship for the VB structures is analogous to the Mulliken population analysis in MO theory at the orbital level.

3. Results and Discussion

Table 1 summarizes the GVB and VBSCF calculated Si−F bond distances values of energy minima (R_e), dissociation energies (D_e), and dipole moments (μ) at R_e and the VB structure weights according to eq 2. Results for all three methods (AE/AE, CEP/AE, and CEP/CEP) at the four theory levels (L-SODS, D-SODS, L-BOVB, and D-BOVB) are presented in Table 1. Figures 1 and 2 show the binding energy curves for the ground electronic state (SiH_3F) and the covalent (SiH_3:F) and dominant ionic ($SiH_3^+F^-$) VB structures at the L-BOVB level for the AE/AE and ECP/ECP methods, respectively. The $SiH_3^-F^+$ curves are at much higher energies. The L-BOVB curves in these figures are generally representative of the interfragment distance dependence of the energies for the adiabatic (SiH_3F) state and individual VB structures obtained in this study. As can be seen from these figures, the covalent structure curve does not show a minimum. The calculated energy minima (R_e) and corresponding dissociation energies (D_e) relative to the homolytic $SiH_3^\bullet + F^\bullet$ dissociation asymptotes shown in Table 1 were taken from three or four point fits of the energies bracketing each

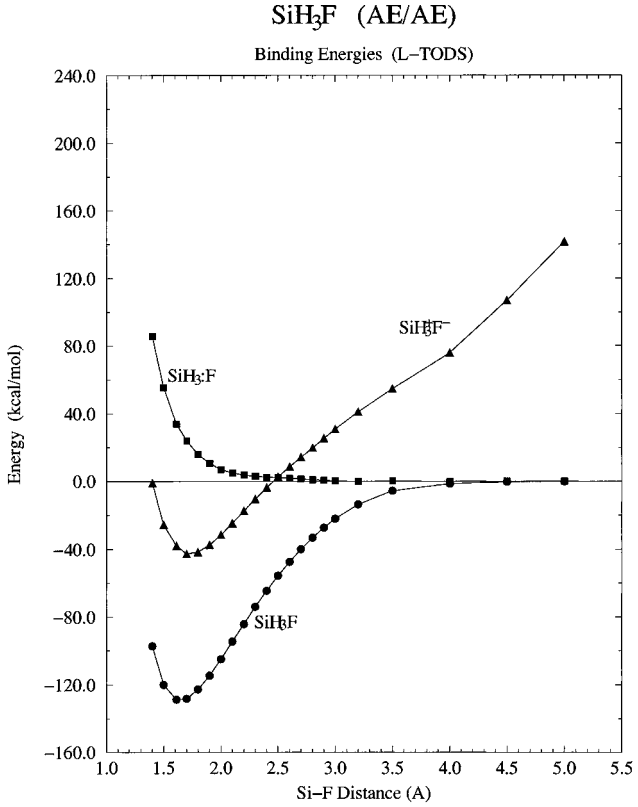

Figure 1. Binding energy curves at the L-BOVB(AE/AE) level.

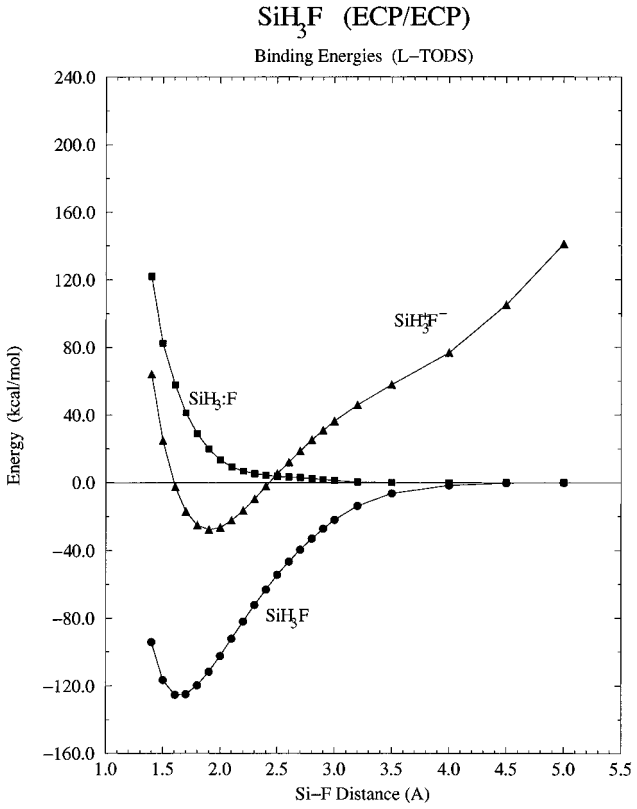

Figure 2. Binding energy curves at the L-BOVB(ECP/ECP) level.

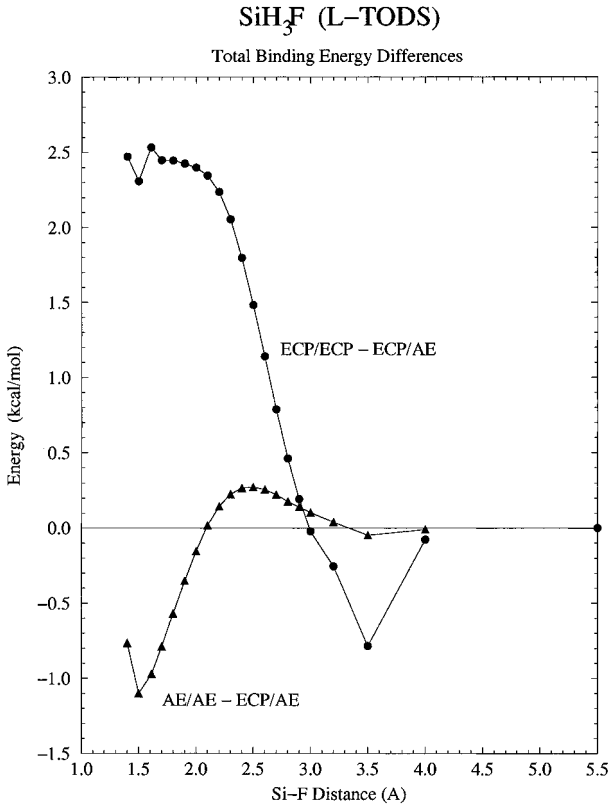

Figure 3. Binding energy difference curves at the L-BOVB level for the adiabatic electronic ground state.

minimum. The calculated points, themselves, are shown in the figures. All the results shown in Table 1 and the figures are taken from the three-configuration VBSCF calculations.

We will first focus on the similarities and differences in the results obtained using the AE and the ECP representations of the core electrons. Using the ECP representation, parallel calculations were carried out with both the ECP and AE basis sets. A comparison between the ECP/ECP and ECP/AE results focuses only on the basis set dependence for the same representation of the core. On the other hand, comparing ECP/AE with AE/AE involves only a difference in the core electron representation using the same basis set. Figure 3 plots these two differences for the electronic ground state SiH_3-F binding energy curve at the L-BOVB model level. This figure shows that the AE/AE-ECP/AE difference has a maximum value of ~1 kcal/mol (near R_e) and decays/oscillates as the interfragment distance increases. The ECP/ECP−ECP/AE difference, on the other hand, hovers at ~2.5 kcal/mol over a wide range of $R(SiH_3-F)$ values, until eventually decaying/oscillating at larger R. Thus, replacing the AE core with the *ab initio* ECP while retaining the AE basis set results in an error of less than 1% in the calculated D_e (see Table 1). On the other hand, using different ECP and AE basis sets with a common ECP representation for the core electrons gives generally larger errors along the whole dissociation path. These results are at the L-BOVB theory level.

A somewhat different picture is obtained at the D-BOVB theory level. For example in Table 1, the calculated ground state dissociation energies at the interpolated values of R_e, which are within 0.002 Å from each other for all three (AE/AE, ECP/AE, and ECP/ECP) methods, the AE/AE−ECP/AE difference is 1.4 kcal/mol, while ECP/ECP−ECP/AE is only 0.4 kcal/mol. A more extensive examination of the D-BOVB BDE curves shows the AE/AE−ECP/AE gap decaying monotonically starting from ~1.8 kcal/mol at $R = 1.4$ Å and decreasing to 0.1 kcal/mol at $R = 2.0$ Å. On the other hand, ECP/ECP−ECP/AE is small (<0.5 kcal/mol) from $R = 1.4$ Å to $R = 1.6$ Å, increases with R thereafter, and reaches a maximum of 1.8 kcal/mol between $R = 2.1$ Å and $R = 2.2$ Å before decaying to zero. This behavior is different from that found at the L-BOVB level shown in Figure 3. Thus, different model levels give somewhat different results with regard to both replacing the core electrons with an ECP and changing the basis set.

The expected R-dependence behavior of the BDE for AE/AE−ECP/AE is a generally increasing difference with decreasing R, as the core region is approached and the ECP approximation becomes increasingly less valid. This is the behavior clearly found at the D-BOVB level, which also gives the most accurate results presented here. The increasing ECP/ECP−ECP/AE differences at the larger R values ($R_e < R < 2.5$ Å), as found at the D-BOVB theory level, could be the result of differences in the specific Gaussian composition of the AE and ECP basis sets, especially for the smaller valued Gaussian exponents. Overall, the relatively small (≤1.8 kcal/mol) variations in the BDE curve incurred by replacing the core electrons by the *ab initio* ECP[16] are generally no greater, and usually somewhat smaller, than the basis set effect at the basis set levels tested here.

Another measure of core representation and basis set dependency can, perhaps, be found in a detailed comparison of the VB energy curves for the individual covalent and ionic structures. These are shown in Figures 4 and 5, respectively, at the L-BOVB model level. Figure 4 shows that the ECP/ECP−ECP/AE energy differences for the SiH_3:F curve are smaller than AE/AE−ECP/AE in the $R \lesssim 2$ Å region, but still reach substantially large values as $R(SiH_3-F)$ decreases. In the analogous comparison for the $SiH_3^+F^-$ structure energy curves (Figure 5) both the ECP/ECP−ECP/AE and AE/AE−ECP/AE differences also show increasingly large values as R gets smaller. Overall in both figures, the AE/AE−ECP/AE curves behave more systematically and as anticipated. The ECP/ECP−ECP/AE differences seem to show different short-range

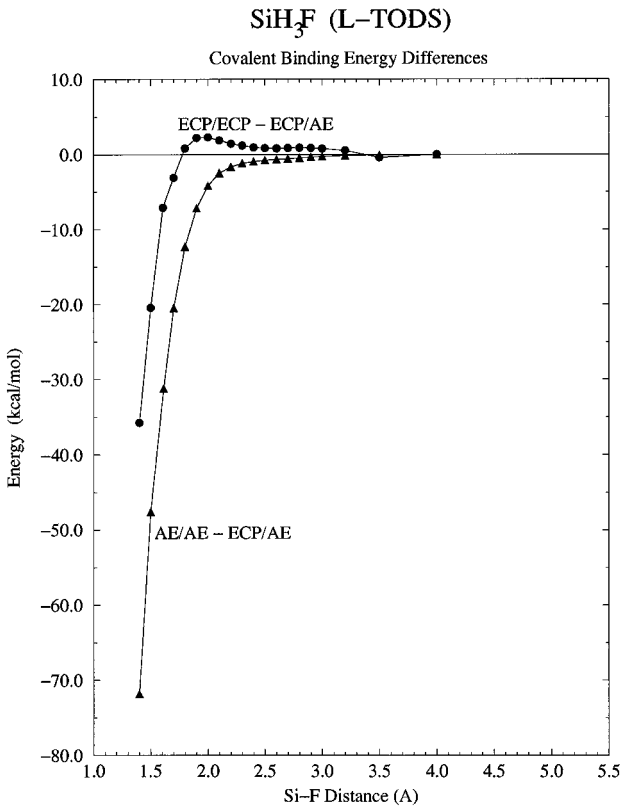

Figure 4. Binding energy difference curves at the L-BOVB level for the VB covalent configuration.

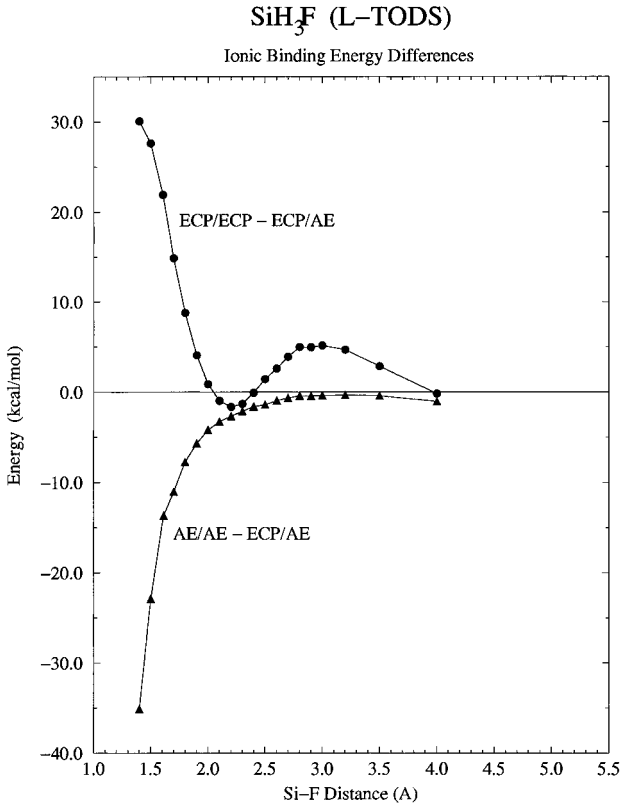

Figure 5. Binding energy difference curves at the L-BOVB level for the VB $SiH_3^+F^-$ configuration.

and long-range behaviors that are indicative of basis set effects. However, what is most significant is that in spite of the large (~36−72 kcal/mol range at $R = 1.4$ Å) AE/AE−ECP/AE and ECP/ECP−ECP/AE energy differences for the individual structures (Figures 4 and 5), the resultant electronic ground state curves show energy differences for the same quantities that are

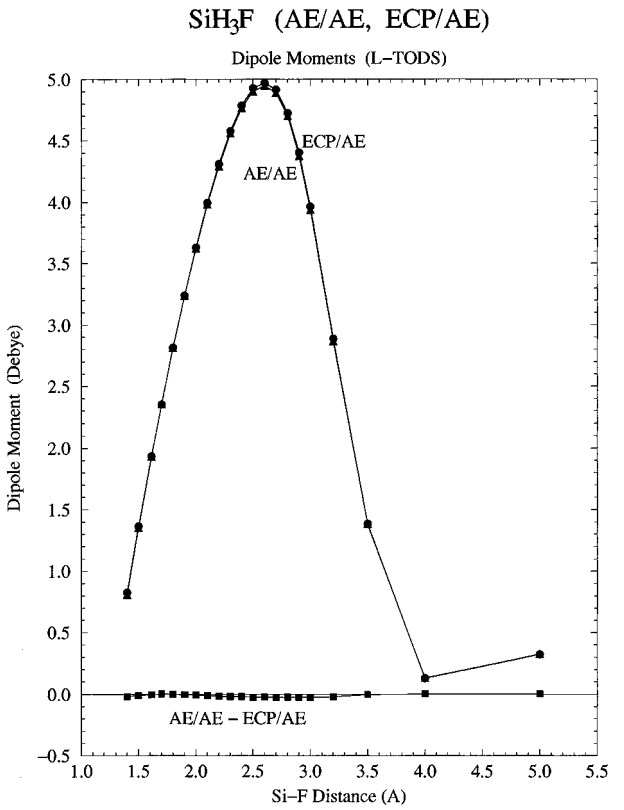

Figure 6. Dipole moment functions and difference curve at the L-BOVB level using the AE basis set for the adiabatic electronic ground state.

more than an order of magnitude smaller, as shown in Figure 3 and Table 1. Thus, core representation and basis set can significantly affect the individual diabatic contributions without seriously affecting observable quantities such as R_e and D_e.

A similar conclusion can be reached by examining the behavior of the calculated ground state dipole moment functions at the L-BOVB level, shown in Figures 6 and 7. The AE/AE−ECP/AE differences (Figure 6) are essentially zero along the whole SiH_3−F bond distance range, while the ECP/ECP−ECP/AE differences are negligible out to 3.0 A, independent of the large differences in the individual energies of the constituent covalent and ionic structures shown in Figures 4 and 5.

The calculated values of R_e, D_e, and μ for SiH_3−F are compared with experiment[12,32,34] in Table 1. The results in this table show that irrespective of the specific combination of core representation and basis set, passive electron delocalization is needed to achieve good accuracy for R_e. Thus, with regard to this property, D-SODS and D-BOVB are closer to experiment than L-SODS or L-BOVB, and D-SODS gives better results than L-BOVB. This latter order of reliability is opposite the result for bond dissociation energies (D_e), where L-BOVB is both larger than D-SODS and closer to experiment. This latter is also the same (absolute value) ordering of total energies since at all four theory levels SiH_3−F dissociates to the same $SiH_3^\bullet$ + F$^\bullet$ radical fragment wave functions and energies. The same conclusions with regard to calculated R_e and D_e values at different theory levels have been reached previously for CH_3−X (X = F, OH, NH_2, CH_3, BH_2, NO, and CN) systems.[10]

The calculated dipole moments shown in Table 1 show that, like for the R_e values, passive electron delocalization is more important than using different orbitals for different VB structures (BOVB), although both improvements are necessary to achieve quantitatively accurate results. The highest level theory used here, D-BOVB, is still 0.16 D above experiment.[34] Like the calculated values of R_e and D_e compared to experiment,[32,33] most

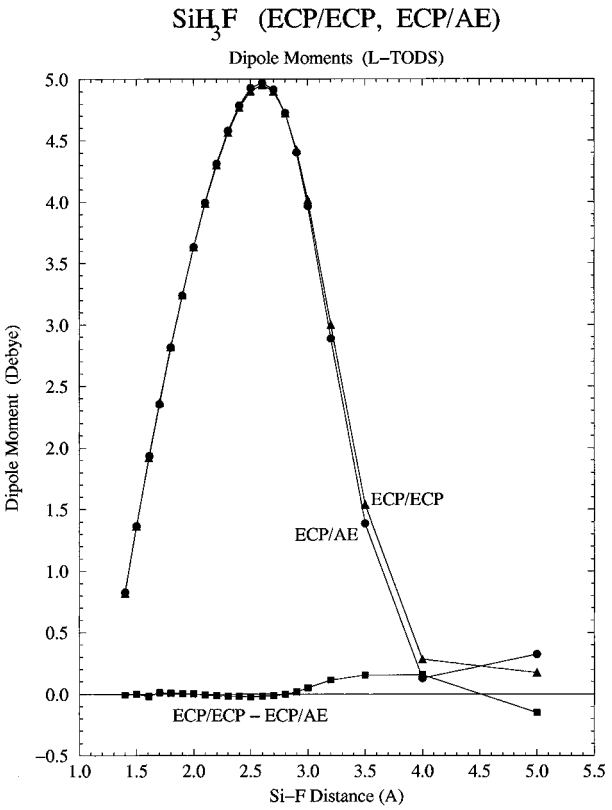

Figure 7. Dipole moment functions and difference curve at the L-BOVB level using the ECP for the adiabatic electronic ground state.

of the residual error is probably due to the need for a larger basis set. For example, all-electron CCSD(T) energies[20] using MP2 optimized geometries in the same AE basis set used here gives a SiH_3-F BDE of 142.2 kcal/mol,[35] close to the D-BOVB-(AE/AE) value in Table 1 of 143.0 kcal/mol. These calculated values of D_e do not include some 4 kcal/mol of zero-point energy (ZPE) and temperature dependent differences that must be subtracted from the electronic BDE for a direct comparison with the experimental D_o.[12] The relatively small value of the dipole moment at R_e is due to the hydrogen atoms in the silylium cation being oppositely charged from the Si atom, forming a counterlever to the Si($\delta+$)−F ($\delta-$) polarity and, therefore, is not indicative of the degree of ionicity of the Si−F bond.

A most interesting aspect of the SiH_3F system in terms of a VB analysis is the behavior of the individual covalent (SiH_3:F) and ionic ($SiH_3^+F^-$) configuration energy curves. As shown in Figures 1 and 2, each of the covalent configuration curves, taken as the appropriate diagonal energy in the relevant three-configuration VBSCF calculation, shows no energy minimum. This interesting result was tested at the fragment localized AE/AE level by generating the binding energy curve for the covalent configuration alone. The resultant curve shows a very shallow energy minimum out at $R \approx 2.10$ Å of only 1.2 kcal/mol, and the curve is still repulsive in the neighborhood of the calculated R_e values in Table 1. At the GVB R_e value, for example, the energy of the directly calculated covalent structure is lowered relative to its diagonal energy value in the three-configuration calculation [L-BOVB(AE/AE)] by 29.2 kcal/mol; but this stabilization is not enough to make it bound relative to the covalent asymptote at $\sim R_e$.

Therefore, in common with the previous CH_3-F study[10] the covalent structure curve in SiH_3-F is generally near-repulsive. However, in contrast to CH_3-F, the ionic $SiH_3^+F^-$ energy curve (Figures 1 and 2) lies below SiH_3:F out to ∼2.5 Å, where the two curves cross without a barrier and the covalent structure continues lower out to the $SiH_3^\bullet + F^\bullet$ dissociation limit, as expected. The lower energy of the ionic curve in the equilibrium distance region ($R \approx 1.6-1.7$ Å) results in the weight of the ionic structure being larger than the weight of the covalent structure by about 50% in the neighborhood of R_e (Table 1). This result is independent of the theory level or method (core representation/basis set) of calculation.

The $SiH_3^+F^-$ ionic state energy in the neighborhood of R_e is also below the $SiH_3^\bullet + F^\bullet$ dissociation limit and, therefore, has an endothermic binding energy relative to the homolytic dissociation asymptote. However, this binding, as a percentage of the calculated adiabatic ground state binding energy in the three-configuration calculations (Table 1), ranges only from 20% to 40%, depending on the method and theory level. A substantial binding energy variation with theory level is not surprising since, for example, the BOVB model always gives a better description of the higher energy VB structure compared to SODS by optimizing individual VB orbitals for each configuration. Therefore, the weight of SiH_3:F increases on going from SODS to BOVB (Table 1). The relatively modest direct binding energy contribution of the $SH_3^+F^-$ ionic structure to the adiabatic state binding energy in the three-configuration calculations requires that the off-diagonal mixing elements between this ionic, the covalent, and the other ionic structure be substantial. The larger these resonance integrals, the more stabilized the adiabatic ground state. As noted previously,[7,10,11] the bond dissociation energy in these type systems is dominated by the resonance coupling term between the structures, rather than by the stability of the dominant VB structure.

In order to probe the form of the directly calculated $SiH_3^+F^-$ energy curve, the single ionic configuration energy curve was also obtained at the fragment localized AE/AE level. At the R_e value for the GVB curve, which corresponds closely to the direct ionic curve energy minimum, the binding energy relative to the covalent dissociation asymptote is 76.6 kcal/mol. This value is still considerably smaller than the total binding energy at the L-BOVB(AE/AE) level of 129.2 kcal/mol, but is larger than the 42.9 kcal/mol binding of the $SiH_3^+F^-$ diagonal energy in the three-configuration calculation (Table 1).

As noted above and shown in Figures 1 and 2, the covalent structure curve in the three-configuration calculations is repulsive, as has been found also for CH_3-F.[10] The difference between SiH_3-F (Table 1) and CH_3-F with regard to covalent/ionic composition within the VB framework is the interchange of the relative weights (eq 2) for these two configurations between the two molecular systems. The $SiH_3^+F^-/SiH_3$:F ratio of weights is approximately the same as the CH_3:F/$CH_3^+F^-$, each at their respective equilibrium bond lengths. In the latter case the covalent CH_3:F energy curve is uniformly below $CH_3^+F^-$, while in SiH_3-F the ionic structure energy curve is below that of SiH_3:F out to ∼2.5 Å. The origin of the dissociative form of the CH_3:F-type energy curves has been attributed, among other explanations, to a repulsive interaction between the fluorine atom lone pair electrons and the C−H bonding electrons.[3] On the basis of this argument alone the repulsiveness of the SiH_3:F curve would be expected to be proportionately smaller than for CH_3:F, each at their respective R_e distances, due to the longer Si−F and Si−H equilibrium bond lengths. This, in fact, is not found here, and at their respective equilibrium geometries the SiH_3:F energy is about 8 kcal/mol less stable than CH_3:F at the L-BOVB(AE/AE) levels. This gap increases at the higher D-BOVB theory level, but the covalent/ionic characterization here is not completely unambiguous. Direct calculation of the single covalent configurations for SiH_3:F and CH_3:F does show the former less repulsive than the latter near their respective R_e values, but by only ∼2.5 kcal/mol. This is a relatively small energy difference compared to

the bond length (0.21 A) and binding energy differences (43.1 kcal/mol) between the two molecules.

Another argument attributes the weakness of the covalent A:F bond to a destabilizing two-orbital, three-electron interaction between the doubly occupied F atom 2s electrons and the same-symmetry covalent bonding electron on A.[3] This repulsion effect would also be expected to diminish proportionately with increasing A−F distance, which is not clearly found here, as noted above. A recent refinement of this last approach[24] attributes the weakness of the covalent structure instability (in H−F, for example) to a destabilizing s−p hybridization on the fluorine atom induced by the A group, relative to the asymptotic unhybridized F atom. Although an intraatomic effect, this differential hybridization mechanism is also expected to be somewhat distance dependent, as found for each A:F energy curve for a given A group (ref 10 and Figures 1 and 2 here). This distance dependence should also show up comparing different A groups such as CH_3 and SiH_3. The *R* dependence of the SiH_3:F structure energy compared to CH_3:F merits further investigation. The individual covalent and ionic VB structures are diabatic-like states based on asymptotic composition, and their energies at other distances along the A−F coordinate are generally not observable. Therefore, a discussion of the bonding mechanism in the purely covalent structure is meaningful only within the framework of the specific VB model being applied.

The inverse relative weights of the covalent and ionic structures for CH_3−F and SiH_3−F raise the question of the proper description of the latter molecule as covalent or ionic. Within the framework of the VB method and the majority weight of the ionic VB structure on the total wave function, the charge distribution in SiH_3−F is ionic, representing a large degree of charge separation between the Si and F atoms. In fact, since the Si−H bonds in the SiH_3 group are polarized toward the hydrogen atoms, the atomic charge on Si is about 50% larger and of opposite sign than on the fluorine atom.[12] At the L-BOVB(AE/AE) level the charge on the fluorine atom is calculated to be $-0.62e$. However, atomic charges are not observables, and the difficulty in finding R_3Si^+ ions either in solution or in the solid state has been invoked as indicating that silyl compounds are generally not ionic.[11] Of course, behavior in solution and in the solid state with regard to $R_3Si^+X^-$ heterolysis is the result of competition between the R_3Si−X bond energy and the other interactions, with solvent molecules in solution, or with other R_3Si−X units or their components in the solid state.[36−39] Silyl compounds have high binding energies when attached to electronegative atoms such as oxygen, nitrogen, or fluorine.[12,38] The binding energy of an acetonitrile solvent molecule to Me_3Si^+ in solution has been calculated to be ∼40 kcal/mol with covalent bonding characteristics for the Si−N bond.[37] The low-temperature crystal structure of SiH_3F shows a significant Si···F nonbonded interaction.[38] After taking account of all the condensed phase interactions, in the balance it may very well be that R_3Si−X will prefer to remain molecular even though its internal charge distribution shows a large charge separation between the R_3Si and X groups.[40,41] In the case of SiH_3−F the large binding energy is not directly due to the ionic character of the Si−F bond but rather to a strong resonance interaction between the ionic and covalent bonding structures.[7,10,11]

At the simplest VB theory level (L-SODS) the calculated bond dissociation energy (Table 1) of SiH_3−F is already 108.2 kcal/mol (AE/AE method). At the same theory level the calculated CH_3−F binding energy is calculated to be only 77.0 kcal/mol.[10] Thus, the large observed increase in the MH_3−F BDE of ∼43 kcal/mol on going from M = C to M = Si already finds at least partial expression (∼29 kcal/mol) even at the lowest theory level. The asymptotic $MH_3^+ + F^-$ ion energies lie above the corresponding $MH_3^\bullet + F^\bullet$ covalent dissociation limits by the difference between the ionization potential (IP) of MH_3 and the electron affinity (EA) of the fluorine atom. In comparing CH_3−F and SiH_3−F, this difference reduces to the difference in IP of the methyl and silyl radicals which is ∼39 kcal/mol.[34] The $SiH_3^+F^-$ asymptote is, therefore, ∼39 kcal/mol closer to its covalent dissociation limit than $CH_3^+F^-$, and the SiH_3−F BDE is larger by ∼43 kcal/mol than CH_3−F. In MH_3−Cl the BDE for M = silicon is larger than for M = carbon by only 23.4 kcal/mol,[11] although the asymptotic covalent−ionic energy gap difference is still ∼39 kcal/mol. Clearly, then, a number of factors contribute to BDE trends in these systems.[11,24] Although the role of the covalent−ionic resonance interaction is significant in these systems, the energy gap between them and its interfragment distance dependence must also play an important part in determining the resultant ground state BDE and their trends. These aspects will be examined in a subsequent study.

One aspect of the SiH_3−F calculations could be of general interest and relevance to the realm of semiempirical VB methods.[42−45] The Wolfsberg−Helmholz formula,[46]

$$H_{12} = KS_{12}[H_{11} + H_{22}]/2 \qquad (3)$$

has been used to obtain the Hamiltonian coupling matrix element, H_{12}, between VB structures such as the covalent (diagonal energy H_{11}) and dominant ionic (H_{22}) configurations. S_{12} is the overlap integral between the two structures, and *K* is a parameter whose value is usually obtained by comparison with some experimental quantity for a known system. Unfortunately, this latter approach is not always feasible, and there is a need to know the theoretical value of the proportionality constant *K*. Equation 3 has been applied here to obtain theoretical values of *K* as a function of the $R(SiH_3$−F) distances for various methods and theory levels, using the calculated VBSCF values of H_{11}, H_{22}, S_{12}, and H_{12}. The interesting result is that $K(R)$ is very constant. For example, at the L-SODS(AE/AE) level the average value of $K(\bar{K})$ from $R = 1.40$ Å to $R = 5.00$ Å is 1.0012, with a maximum error of 0.0002 over the 22 points sampled (Figures 1 and 2). The analogous result for L-BOVB(AE/AE) is $\bar{K} = 1.0009$, again with a maximum error of 0.0002 out to $R = 3.20$ Å and 0.0004 out to $R = 5.000$ Å. At the BOVB theory level VBSCF at the larger *R* values can be problematic since the electronic ground state essentially coincides with the covalent configuration, and the ionic structure, which then contributes negligibly to the adiabatic ground state wave function in these regions, is almost indeterminate as a canonical $SiH_3^+F^-$ electronic structure. The L-SODS(ECP/ECP) level gives a $\bar{K}$ value of 1.0164, with a larger maximum deviation of 0.0030 at the shorter *R* distances, as expected for the ECP method/basis. The average calculated value of K using the L-SODS(ECP/AE) model is 1.000 91, with a maximum error of 0.0005 over the same 22 point grid of SiH_3−F distances. In summary, eq 3 gives an excellent account of the resonance interaction integrals H_{12} and its distance dependence with a fixed value of *K* that is almost exactly equal to 1.0.

4. Summary

Existing *ab initio* effective core potentials that replace the inert atomic core electrons and accompanying valence electron basis sets have been used in VBSCF theory to calculate the homolytic bond dissociation energy curves of SiH_3−F. Four VB theory levels have been applied that involve both the same and tailored orbitals for different VB structures, and both with and without passive electron delocalization between the SiH_3

and F fragment orbitals. Several core representation/basis set combination methods have been tested, ECP/ECP, ECP/AE, and AE/AE, for comparison purposes. It is found that different model levels give somewhat different results with regard to both replacing the core electrons with an ECP (AE/AE-ECP/AE) and changing basis sets (ECP/ECP-ECP/AE). However, the variation in bond dissociation energy curves for the adiabatic ground state incurred by using the ECP is generally smaller than the basis set effect at the basis set levels used here. The individual covalent and ionic VB configuration energy curves show variations with core representation and basis set that are more than an order of magnitude larger than for the adiabatic ground state. The highest VBSCF theory level applied here, D-BOVB, shows a systematic and predictable behavior for both core representation and basis set dependency of the bond dissociation energy curves. A comparison of calculated R_e, D_e, and dipole moment values with experiment shows, again, that the D-BOVB theory level is required for quantitative accuracy.

The VB energy dissociation curves of SiH_3-F for the three-configuration calculations show that the ionic configuration ($SiH_3^+F^-$) lies below the covalent (SiH_3:F) configuration from R(Si−F) below R_e out to R(Si−F) ≈ 2.5 Å, where the two curves cross without a barrier and the covalent configuration continues lower out to the ground state $SiH_3^\bullet + F^\bullet$ dissociation limit. The lower energy of the ionic structure curve in the neighborhood of R_e results in the weight of $SiH_3^+F^-$ being ∼50% larger than the weight of SiH_3:F at R_e. The ionic structure energy at R_e is bound relative to the ground state asymptotes but contributes only 20−40% of the total ground state binding energy, depending on theory level. Thus, the off-diagonal resonance interaction (H_{12}) between the covalent and ionic configurations essentially determines the magnitude of D_e in SiH_3-F.

The covalent structure energy curve is near-repulsive along the whole range of R(Si−F) values. The same has been found previously for CH_3-F and other systems.[7,1011] Conventional explanations for the lack of VB covalent structure binding in A−F-type systems generally involve a destabilizing A-induced 2s−2p orbital mixing on the fluorine atom. Such an interaction would be expected to be R(A−F) dependent, as shown by the individual SiH_3:F and CH_3:F curves. However, it is calculated here that the stabilization relative to asymptotes is, at best, only marginally greater for SiH_3:F at its R_e (1.59 Å) than for CH_3:F at its R_e (1.38 Å).

The proportionality constant K in the equation $H_{12} = KS_{12}[H_{11} + H_{22}]/2$, where H_{ij} and S_{ij} ($i, j = 1, 2$) are the Hamiltonian and overlap matrix elements, respectively, involving the covalent and lowest energy ionic configurations, has been evaluated using the results of these calculations. At the L-SODS theory level, K is found to be very close to 1 and remarkably constant over the range of R(Si−F) distances sampled here, independent of core representation and basis set.

Acknowledgment. This work was supported by a grant from the Israel Science Foundation (484/95).

References and Notes

(1) Pauling, L. *The Nature of the Chemical Bond*, 3rd ed.; Cornell University Press: Ithaca, New York, 1960.
(2) Cooper, D. L.; Gerratt J.; Raimondi, M. *Adv. Chem. Phys*. **1987**, *68*, 319; *Chem. Rev*. **1991**, *91*, 929.
(3) Hiberty, P. C.; Flament, J. P.; Noizet, E. *Chem. Phys. Lett*. **1992**, *189*, 259; Hiberty, P. C.; Humbel, S.; Byrman, C. P.; van Lenthe, J. H. *J. Chem. Phys*. **1994**, *101*, 5969.
(4) Bobrowicz, F. W.; Goddard, W. A., III, in, *Methods of Electronic Structure Theory*; Schaeffer, H. F., III, Ed.; Plenum Press: New York, Vol. 3, 1977.
(5) Mo, Y.; Zhang, Q. *J. Chem. Phys*. **1995**, *99*, 8535. Mo, Y.; Lin, Z.; Wu, W.; Zhang, Q. *J. Phys. Chem*. **1996**, *100*, 6469.
(6) Basch, H.; Aped, P.; Hoz, S. *Chem. Phys. Lett*. **1996**, *255*, 336.
(7) Sini, G.; Maitre, P.; Hiberty, P. C.; Shaik, S. *J. Mol. Struct*. **1991**, *229*, 163. Shaik, S.; Maitre, P.; Sini, G.; Hiberty, P. C. *J. Am. Chem. Soc*. **1992**, *114*, 7861.
(8) Hoz, S.; Basch, H. *J. Am. Chem. Soc*. **1992**, *114*, 4364.
(9) McWeeny, R. *J. Chem. Phys*. **1994**, *101*, 4826.
(10) Basch, H.; Aped, P.; Hoz, S. *Mol. Phys*. **1996**, *89*, 331.
(11) Lauvergnat, D.; Hiberty, P. C.; Danovich, D.; Shaik, S. *J. Phys. Chem*. **1996**, *100*, 5715.
(12) Basch, H.; Hoz, T. In *The Chemistry of Organic Germanium, Tin Lead Compounds*; Patai, S., Ed.; Wiley & Sons Ltd.: Chichester, U.K. 1995; Chapter 1.
(13) Jasinski, J. M.; Becerra, R.; Walsh, R. *Chem. Rev*. **1995**, *95*, 1203, and references therein.
(14) Kahn, L. R.; Baybutt, P.; Truhlar, D. G. *J. Chem. Phys*. **1976**, *65*, 3826.
(15) For a review see: Gropen, O. *Methods in Computational Chemistry*; Wilson, S., Ed.; Plenum; New York, 1988; Vol. 2, Chapter 3.
(16) Stevens, W. J.; Basch, H.; Krauss, M. *J. Chem. Phys*. **1984**, *81*, 6026.
(17) Stevens, W. J.; Basch, H.; Krauss, M.; Jasien, P. G. *Can. J. Chem*. **1992**, *70*, 612.
(18) Verbeek, J.; Lengenberg, J.; Byrman, C. P.; Van Lenthe, J. H. *TURTLE− An Ab initio VB/VBSCF/VBCI Program*; Theoretical Chemistry Group, Debye Institute: University of Utrecht, 1995.
(19) Van Lenthe, J. H.; Balint-Kurti, G. G. *Chem. Phys. Lett*. **1980**, *76*, 138; *J. Chem. Phys*. **1983**, *78*, 5699.
(20) Frisch, M. J.; Trucks, G. W.; Schlegel, H. B.; Gill, P. M. W.; Johnson, B. G.; Robb, M. A.; Cheeseman, J. R.; Keith, T. A.; Petersson, G. A.; Montgomery, J. A.; Raghavachari, K.; Al-Laham, M. A.; Zakrzewski, V. G.; Ortiz, J. V.; Foresman, J. B.; Cioslowski, J.; Stefanov, B. B.; Nanayakkara, A.; Challacombe, M.; Peng, C. Y.; Ayala, P. Y.; Chen, W.; Wong, M. W.; Andres, J. L.; Replogle, E. S.; Gomperts, R.; Martin, R. L.; Fox, D. J.; Binkley, J. S.; Defrees, D. J.; Baker, J.; Stewart, J. P.; Head-Gordon, M.; Gonzalez, C.; Pople, J. A. *Gaussian 94* (Revision C), Gaussian, Inc.: Pittsburgh, PA, 1995.
(21) Huzinaga, S. *J. Chem. Phys*. **1965**, *42*, 1293.
(22) Dunning, T. H. *J. Chem. Phys*. **1975**, *55*, 116.
(23) Krishnan, R.; Binkley, J. S.; Seeger, R.; Pople, J. A. *J. Chem. Phys*. **1980**, *72*, 650.
(24) Lauvergnat, D.; Maitre, P.; Hiberty, P. C.; Volatron, F. *J. Phys. Chem*. **1996**, *100*, 6463.
(25) Hiberty, P. C.; Humbel, S.; Archirel, P. *J. Phys. Chem*. **1994**, *98*, 11697.
(26) Verbeek, J. *Nonorthogonal Orbitals in Ab Initio Many-Electron* Wavefunctions, Ph.D. Thesis, Utrecht University, Utrecht, Holland, 1990.
(27) Ghailane, R.; Lepetit, M.-B.; Malrieu, J.-P. *J. Phys. Chem*. **1993**, *97*, 94.
(28) Voter, A. F.; Goddard, W. A., III. *Chem. Phys*. **1981**, *57*, 253; *J. Chem. Phys*. **1986**, *75*, 3638; *J. Am. Chem. Soc*. **1986**, *108*, 2830. M. Goodgame, M. A.; Goddard, W. A., III. *Phys. Rev*. **1985**, *54*, 661.
(29) Langenberg, J. H.; Ruttink, P. J. A. *Theor. Chim. Acta* **1993**, *85*, 285.
(30) Byrman, C. P. Nonorthogonal Orbitals in Chemistry. Ph.D. Thesis, Utrecht University, Utrecht, Holland, 1995.
(31) Chirgwin, B. H.; Coulson, C. A. *Proc. R. Soc. London Ser. A* **1950**, *201*, 196.
(32) Robiette, A. G.; Georghion, C.; Baker, J. G. *J. Mol. Spectrosc*. **1976**, *63*, 391.
(33) Calculated from: Lias, S. G.; Bartmess, J. E.; Liebman, J. F.; Holmes, J. L.; Levin, R. D.; Mallard, W. G. *J. Phys. Chem. Ref. Data*, **1988**, *17*, Suppl. 1.
(34) *Handbook of Chemistry Physics*; Lide, D. R., Ed.-in-Chief, 1995−1996, *76*, pp 9−43.
(35) Basch, H. *Inorg. Chim. Acta* **1996**, *252*, 265.
(36) Schleyer, P. v. R.; Buzek, P.; Muller, T.; Apeloig, Y.; Siehl, H.-U. *Angew. Chem., Int. Ed. Engl*. **1993**, *32*, 1471.
(37) Basch, H. *Inorg. Chim. Acta* **1996**, *242*, 191.
(38) Arshadi, M.; Johnels, D.; Edlund, H.; Ottoson, C.-H.; Cremer, D. *J. Am. Chem. Soc*. **1996**, *118*, 5120.
(39) Blake, A. J.; Ebsworth, E. A.; Henderson, S. G. D.; Welch, A. J. *Acta Crystallogr*. **1985**, *C41*, 1141.
(40) Gronert, S.; Glaser, R.; Streitwieser, A. *J. Am. Chem. Soc*. **1989**, *111*, 3111.
(41) Shi, A.; Boyd, R. J. *J. Phys. Chem*. **1991**, *95*, 4698.
(42) Aqvist, J.; Warshel, A. *Chem. Rev*. **1993**, *93*, 2523.
(43) Chang, V.; Miller, W. H. *J. Phys. Chem*. **1990**, *94*, 5884.
(44) Shaik, S.; Hiberty, P. C. *Adv. Chem. Phys*. **1995**, *26*, 99.
(45) Gill, P. M. W.; Radom, L. *Chem. Phys. Lett*. **1988**, *147*, 213.
(46) Wolfsberg, M.; Helmhotz, L. *J. Chem. Phys*. **1952**, *20*, 837.